Journal of Applied Polymer Science

Development of thermally conductive polymer matrix composites by foaming-assisted networking of micron- and submicron-scale hexagonal boron nitride

Hao Ding, Yanting Guo, Siu Ning Leung
Department of Mechanical Engineering, Multifunctional Materials/Micro-and-Nanostructuring Laboratory, Lassonde School of Engineering, York University, Toronto M3J 1P3, Canada
Correspondence to: S. N. Leung (E-mail: sunny.leung@lassonde.yorku.ca)

ABSTRACT: Thermally conductive polymer matrix composite (PMC) foams with effective thermal conductivities (k_{eff}) higher than their solid counterparts have been developed for the first time. Using a material system consists of low density polyethylene and micron-scale or submicron-scale hexagon boron nitride platelets as a case example, this article demonstrates that foaming-assisted filler networking is a feasible processing strategy to enhance PMC's k_{eff}, especially at a low hBN loading. Parametric studies were conducted to identify the structure-to-property relationships between foam morphology (e.g., cell population density, cell size, and foam expansion) and the PMC foam's k_{eff}. In particular, there exists an optimal cell size to maximize the PMC foam's k_{eff} for foams with up to 50% volume expansion. However, an optimal cell size is absent for PMC foams with higher volume expansion. X-ray diffraction (XRD) analyses reveal that both the presence of hBN platelets and foam expansion promoted the crystallization of LDPE phase. Moreover, the XRD spectra also provide evidence for the effect of foam expansion on the orientation of hBN platelets. Overall, the findings provide new directions to design and fabricate thermally conductive PMC foams with low filler contents for heat management applications. © 2015 Wiley Periodicals, Inc. J. Appl. Polym. Sci. **2016**, *133*, 42910.

KEYWORDS: composites; conducting polymers; foams; morphology; structure-property relations

Received 5 May 2015; accepted 4 September 2015
DOI: 10.1002/app.42910

INTRODUCTION

Transistor density on an integrated circuit has rapidly increased in the past 50 years.[1] By virtue of the emerging three-dimensional (3D) chip architecture, this trend is expected to continue for at least another decade.[2] Such technology advancement provides an opportunity to fabricate powerful and miniaturized processors. However, the improved performances of components with smaller footprints also mean dramatic increases in their heat density. In order to avoid the hardware failure caused by excessive heat accumulation, new thermally conductive electronic packaging materials for fast heat dissipation are in great demands. In the interest of superior electrical insulating property, low cost, light weight, and good processability, polymers (e.g., epoxy) have been widely used as traditional integrated circuit packaging materials.[3] However, their low thermal conductivities limit their heat transfer rates, leading to unsatisfactory performance in dissipating heat for new electronic devices. Therefore, the development of new thermally conductive polymer matrix composites (PMC) without compromising the aforementioned benefits of polymers would be welcomed by electronics manufacturers. In this context, active research and development have been conducted to design thermally conductive PMC.[4–9]

Thermally conductive PMC are often fabricated by embedding thermally conductive fillers into polymer matrices. Commonly used fillers include metal,[4,5] ceramic,[6,7] and carbon-based fillers.[8,9] PMC's effective thermal conductivity (k_{eff}) is predominantly determined by the content and intrinsic thermal conductivity of the fillers. When restricting filler loadings to 33.3 vol % or below, PMC's k_{eff} were reported to be slightly above 2.0 W m^{-1} K^{-1}.[10] Although literatures revealed that PMC's k_{eff} can further be promoted by increasing the loadings of thermally conductive filler beyond 50 vol %,[10–12] high filler loading would significantly compromise some key benefits of using polymers for electronic packaging. For instance, fillers generally have higher density and are more expensive than polymers. Excessive use of filler would be an impediment to maintain the final product's light weight and low cost. Moreover, the increased melt viscosity brought by high filler loadings would be detrimental to the processing of PMC. Therefore, new design

and fabrication strategies of thermally conductive PMC loaded with minimum filler contents would be crucial.

Intuitively, one potential strategy to promote PMC's k_{eff} is to use filler with the highest possible thermal conductivity. However, Bigg showed that when the ratio between filler's and polymer matrix's thermal conductivities exceeds 1000, further increase in filler's thermal conductivity has negligible effect on the k_{eff} of composites.[13] As a result, the inclusion of carbon-based fillers with extremely high intrinsic thermal conductivity (e.g., carbon nanotubes and exfoliated graphite nanoplatelets) in PMC failed to significantly increase PMC's k_{eff}.[14,15] This limitation was commonly believed to be attributed to the phonon scattering at the imperfect connections of the filler-polymer and/or filler-filler interfaces.[16,17] As a result, these PMC were unable to take full advantage of the carbon-based fillers' high intrinsic thermal conductivities. To circumvent this challenge, it is important to facilitate the development of thermally conductive filler network in a polymer matrix by some micro-and-nanostructuring techniques (e.g., electric field-induced filler alignment,[18] ultra-drawing,[19] ultra-sonication,[20] and foaming,[21] etc.). Using electric field to align multi-wall carbon nanotubes (MWCNT) in epoxy resin, Martin *et al.* obtained composites that were suitable for electrostatic dissipation.[18] The observed orientation of the field-induced nanotube networks also showed promising optical transparency. In a study of liquid crystal polymer (LCP)-graphene nanoplatelets (GNP) nanocomposite, Leung *et al.* found that ultra-drawing of LCP-GNP nanocomposite would enhance alignment of LCP fibrils and the embedded GNP, which increases the k_{eff} of the nanocomposite.[19] Yu *et al.* used ultra-sonication to disperse hybrid single wall carbon nanotube (SWCNT)-GNP in epoxy.[20] With the formation of thermally conductive filler network by hybrid one-dimensional (1D) and two-dimensional (2D) fillers, they were able to fabricate PMC that achieved k_{eff} of 3.35 W m^{-1} K^{-1} with only 20 wt % of filler. Extensive studies reported the preparation of various solid PMC,[22–25] as well as porous PMC with enhanced properties.[21,26–28] In particular, Okamoto *et al.* demonstrated that foaming-induced biaxial flow aligned clay particles along the cell boundary in a polypropylene matrix, which would suppress cell rupture.[21] Experimental studies have shown that foaming enhanced 3D filler networking would result in the promotion of PMC's mechanical,[21,29] and/or electrical properties.[30,31] As an extension, Chan *et al.* demonstrated that foaming-assisted networking of hBN in linear low density polyethylene composites would help to fabricate novel light-weight thermally conductive PMC.[32] Although PMC foams with k_{eff} higher than their solid counterparts could not be achieved, this work revealed that foaming-induced filler alignment around expanding bubbles helped reduce the PMC's density without significantly compromising their high k_{eff}. In addition, Ding and Leung developed an analytical model to predict PMC foam's k_{eff} by considering the PMC foam system as a thermal resistor network.[33] This model also accounts for the foaming-induced filler alignment in a polymer matrix. It had successfully predicted the trend of how PMC foam's k_{eff} depend on the foam's volume expansion percent. However, without considering the thermal contact resistance at the filler-polymer and filler-filler interfaces, the model could not completely reveal all underlying mechanisms that govern the PMC foam's structure-to-property relationship. In order to fill the technology gap, additional experimental studies are necessary to elucidate the dependence of PMC foam's k_{eff} on the foam morphology (e.g., cell population density, cell size, and foam expansion percent).

Table I. Physical Parameters of LDPE

Property	Value	Unit
Density (ρ)	918	kg/m^3
Melting temperature (T_m)	105–115	°C
Thermal conductivity (k)	0.30–0.34	W m^{-1} K^{-1}
Dielectric strength	27	MV/m

This article aims to fill such technology gap by conducting a comprehensive experimental study of PMC foams' k_{eff} with different filler sizes and foam morphologies. It must be noted that this work represents the first endeavor to develop PMC foams with their k_{eff} higher than solid PMC embedded with the same filler loadings. The concepts demonstrated in this research can easily be extended to other polymer systems as well as foaming processes (e.g., supercritical carbon dioxide physical foaming) to satisfy the needs of specific applications and to reduce manufacturing cost.[34,35] Using low density polyethylene (LDPE)-hexagonal boron nitride (hBN) composite foams blown by Expancel® microspheres as a case example, the effects of filler loading, filler size, volume expansion percent, cell size, and cell population density on PMC foam's k_{eff} were studied parametrically. The revealed structure-to-property relationships would provide guidelines to develop PMC foams with enhanced effective thermal conductivity and low mass density, which are two key properties to promote future electronic devices' heat dissipation and ensure their portability. Furthermore, the reduction of material consumption by foaming would result in more environmentally sustainable polymeric material systems.

EXPERIMENTAL

Materials

Commercially available LDPE (Nova Chemicals, NovaPol, LA-0219-A) was used as the matrix material in this work. Micron-scale and submicron-scale hBN platelets (PolarTherm powder grade PT110 and AC6041) were purchased from Momentive Performance Materials Inc. Expancel® microspheres (Akzonobel, 980 DU 120) were employed as the foaming agent to create cellular structures in the LDPE-hBN composites. Tables (I–III) summarize the physical properties of LDPE, hBN, and Expancel® microspheres, respectively.[36,37] The selection of materials was based on several rationales. Expancel® microspheres are very small spherical particles that consist of a plastic shell encapsulating a gas. Their volume increases dramatically when they are heated to their activation temperature (i.e., soften their shells and increase their internal pressure). Since the activation temperature for expanding Expancel® microspheres is 157 to 173°C, LDPE, which has its melting point lower than the microsphere's onset temperature, was chosen to decouple the melting and foaming processes. hBN micron-scale and submicron-scale

Table II. Physical Parameters of hBN

Property	Value		Unit
	PT110	AC6041	
Density (ρ)	2280	2280	kg/m^3
In-plane thermal conductivity ($k_{//}$)	300+[36,37]	300+[36,37]	W m^{-1} K^{-1}
Through-plane thermal conductivity ($k_{\perp}$)	~3[36,37]	~3[36,37]	W m^{-1} K^{-1}
Lateral size	45	6	μm
Thickness	1–3	0.1–0.5	μm
Specific surface area	0.6	8	m^2/g

platelets, which possess highly anisotropic thermal conductivity, were selected to demonstrate the effect of foaming-assisted filler alignment on the PMC's k_{eff}. Moreover, their relatively low Knoop hardness (i.e., 11 kg/mm^2) and graphite-like layered structure are advantageous for composite processing. The use of Expancel® microspheres as the foaming agent was due to the possibility to precisely control the PMC's foam morphology (i.e., cell population density, cell size, and volume expansion).

Sample Preparation

Table IV summarizes the material composites of the PMC and their foam samples being studied. A previous study found that the dynamic storage modulus of polymer matrix composites filled with hBN platelet increased sharply at hBN loadings closed to 10 vol %, indicating a sudden change in the material structure (i.e., formation of interconnected filler network).[38] As a result, the lowest filler loading studied in this work was chosen to be 9.21 vol %. The overall procedures to prepare PMC samples for the measurements of their k_{eff} are illustrated in Figure 1. Initially, LDPE pellets were ground into fine powders with particle sizes ranging from 250 μm to 500 μm by a mill freezer (SPEX SamplePrep Group, model 6770, Freezer/Mill). Calculated amounts of hBN, LDPE and Expancel® microspheres were weighed and dry-blended by continuous tumbling action at room temperature. The mixtures were then compression-molded into cylindrical samples of 20 mm in diameters and 10 mm in thicknesses by the following procedures:

STEP 1. The dry-blended powders were compacted, by a compression molding machine (Carver Press, 4386 CH), into cylindrical mold cavities at room temperature for 1 min under a pressure of 20 MPa. The compacting step aimed to reduce the chance of undesired void formation within the compression-molded samples.

STEP 2. The compacted mixtures were heated to 125°C at 5 MPa and equilibrated at the set temperature for 25 min to completely melt the LDPE matrix.

STEP 3. The temperature was subsequently raised to 180°C and maintained at that temperature for 5 min to activate the expansion of Expancel® microspheres.

STEP 4. The compression-molded samples were transferred to a cooling module and clamped between a pair of cooling plates with flowing water channels to solidify the samples.

The same procedures were applied to fabricate both solid and foamed PMC samples to ensure all samples experienced the same thermal history. For solid PMC samples, the mold cavities were fully filled with the desired compositions of dry-blended LDPE-hBN mixtures without the addition of Expancel® microspheres. For PMC foam samples, the mold cavities were partially filled to a predefined volume percentage in order to control the volume expansion percent of the samples. Upon the expansion of the microspheres, the partially-filled mold cavity would be completely filled by the expanded material systems. For example, the mold cavities were 50% filled to fabricate PMC foam samples with 100% volume expansion.

The cellular morphology of the PMC foams was precisely controlled by the volume percent of the unfilled mold cavities as well as the amount of Expancel® microspheres. The volume expansion percent of the PMC foam was controlled by the percentage of mold filling. Assuming all microspheres would be

Table III. Physical Parameters of Expancel® 980 DU 120

Property	Value		Unit
	Pre-expansion	Postexpansion	
Density (ρ)	1100	30	kg/m^3
Size	25–40	120	μm
Activation temp.	157–173	–	°C
Shape	Spherical	Spherical	–

Table IV. Material Compositions of PMC Samples being Studied

Filler loading	Volume expansion (%)	Expancel® loading
9.21 vol % hBN$_{AC6041}$	0	n/a
	25	1×, 1.5×, 2.5×, 5×, 10×
	50	1×, 1.5×, 2.5×, 5×, 10×
	75	1×, 1.5×, 2.5×, 5×, 10×
	100	1×, 1.5×, 2.5×, 5×, 10×
9.21 vol % hBN$_{PT110}$	0	n/a
	25	2.5×
	50	2.5×
	75	2.5×
	100	2.5×
27.63 vol % hBN$_{AC6041}$	0	n/a
	25	2.5×
	50	2.5×
	75	2.5×
	100	2.5×

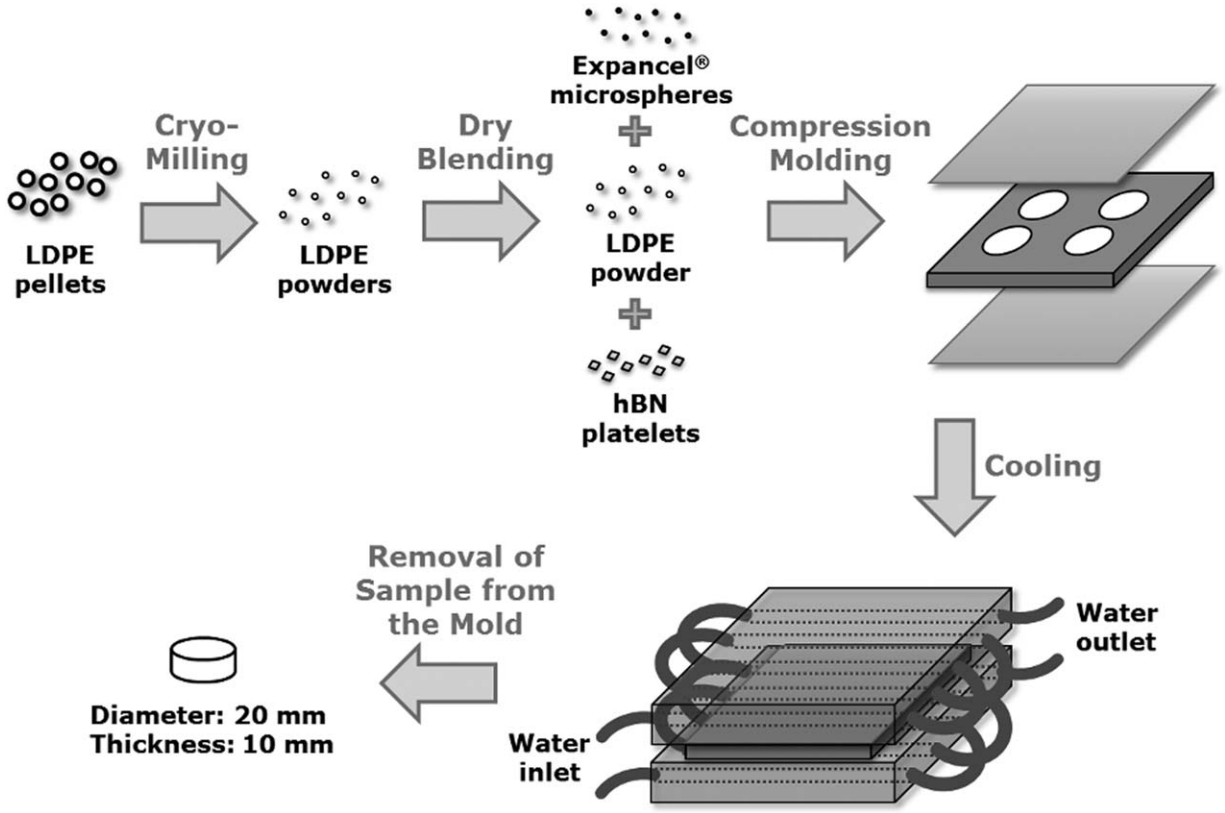

Figure 1. Procedures of sample preparation.

expanded to their maximum sizes (i.e., 120 μm), the minimum loading of Expancel® microspheres can be estimated by eq. (1):

$$m = \frac{V_{\text{void}} d_o^3 \rho}{d_{\text{max}}^3} \quad (1)$$

where m is the minimum required mass of Expancel® microspheres, V_{void} is the volume of the free space in mold (i.e. volume of mold minus total volume of LDPE and hBN), d_o is the diameter of unexpanded microspheres, d_{max} is the maximum diameter upon fully expansion; and ρ is the density of unexpanded Expancel® microspheres (as indicated in Table III).

In order to vary the cell size and/or the cell population density of the PMC foams, the microsphere contents were varied to different multiples (n) of the minimum required amount calculated by eq. (1). In particular, n was varied at 1×, 1.5×, 2.5×, 5×, and 10× to generate PMC foams with different cell population densities and cell sizes. The theoretical average cell sizes for different loadings of microspheres, which are summarized in Table V, can be calculated by eq. (2):

$$d = \frac{d_{\text{max}}}{\sqrt[3]{n}} \quad (2)$$

where d is the theoretical average cell size and d_{max} is the maximum cell size when the microsphere is fully expanded.

Sample Characterization

The hBN's dispersion and/or foam morphology of LDPE-hBN composites and their foams were observed by scanning electron microscopy (FEI Company, Quanta 3D FEG). Samples' cross-sections were exposed by cryofracturing PMC samples under liquid nitrogen. The fractured surface was sputter-coated with gold (Denton Vacuum, Desk V Sputter Coater).

The k_{eff} of LDPE-hBN composites and their foams were measured with a thermal conductivity analyzer (TCA) in accordance to ASTM E1225.[39] The k_{eff} of three samples of each composition were measured for subsequent analyses. The average values and the standard deviations for all compositions were calculated and reported. One-way Analysis of Variance (ANOVA) was employed to test the significance of the dependence of k_{eff} on different parameters related to the PMC foam's cellular morphology. The volume expansion percent (VE %) of PMC foams were determined by eq. (3):

$$\text{VE\%} = \left(\frac{V_{\text{foam}} - V_{\text{solid}}}{V_{\text{solid}}}\right) \times 100\% \quad (3)$$

Table V. Theoretically Calculated Sizes of Expanded Expancel® Microspheres

Multiple of required microspheres loading (n)	Average cell size (μm)
1	120
1.5	104
2.5	88
5	70
10	56

where V_{foam} is the volume of the PMC foam sample and V_{solid} is the volume of the solid portion (i.e., LDPE and hBN) of the sample.

In order to investigate the effects of hBN and foam expansion on the crystalline structure of the LDPE and LDPE composites, X-ray diffraction analyses were conducted using a Philips Analytical X-ray diffractometer equipped with a Cu anode running at 40 kV and 40 mA. The scanning was carried out in an angular region (2θ) ranging from 10° to 60°, with a step size of 0.02°/min and time-per-step of 2 s. The obtained X-ray diffraction spectra were analyzed with X-Pert system software. The crystalline sizes were determined by the Scherrer equation,[40] shown in eq. (4):

$$L = \frac{K\lambda}{\beta \cos\theta} \quad (4)$$

where K is the Scherrer constant, λ is the wavelength of the X-ray, β is the breadth of the diffraction peak, and θ is half of the diffraction angle.

RESULTS AND DISCUSSION

Although PMC can be fabricated by several processing technologies, including melt-compounding and dry-blending, previous studies revealed that dry-blended PMC samples (e.g., polyphenylene sulfide-hBN composites and liquid crystal polymer-hBN composites) yielded higher k_{eff} than those prepared by melt-compounding.[41] Therefore, in this study, both the solid LDPE-hBN mixtures and the foamable LDPE-hBN mixtures were prepared by dry-blending.

Effects of hBN Platelet Sizes and Contents on PMC's k_{eff}

Figure 2 plots the effects of hBN contents on the k_{eff} of solid LDPE-hBN composites filled with either micron-scale hBN platelets (i.e., hBN_{PT110}) or submicron-scale hBN platelets (i.e., hBN_{AC6041}). Regardless of the platelet's size, the PMC's k_{eff} increased with hBN loadings, ranging from 0 vol % to 30 vol %. While the size of hBN platelets showed negligible effect on the PMC's k_{eff} at low hBN loading (e.g., 9.21 vol %), PMC filled with submicron-scale hBN platelets demonstrated more pronounced enhancement on the PMC's k_{eff} at higher hBN loadings (e.g., 18.42 vol % and 27.63 vol %). At low hBN loading, the population density of hBN platelets was not sufficient to establish a thermally conductive network in the LDPE matrix. Therefore, PMC's k_{eff} solely depended on the hBN content. However, hBN platelets were able to form an interconnected network in the LDPE matrix at a high hBN loading. Considering that the specific surface areas for hBN_{PT110} and hBN_{AC6041} are 0.6 m^2/g and 8.0 m^2/g, respectively, the submicron hBN platelet (i.e., hBN_{AC6041}) would have a higher efficiency to form a thermally conductive network. Therefore, the corresponding LDPE-hBN composite's k_{eff} increased more rapidly with higher hBN loadings. Nevertheless, no percolation-like behavior was observed in the relationship between hBN loading and PMC's k_{eff}. This could be attributed to the phonon scattering at the filler-filler interfaces, which is detrimental to heat conduction, despite the establishment of filler network.[16,42] Although the measured k_{eff} of solid PMCs did not show obvious evidence in the formation of thermally conductive hBN network in LDPE-hBN composites

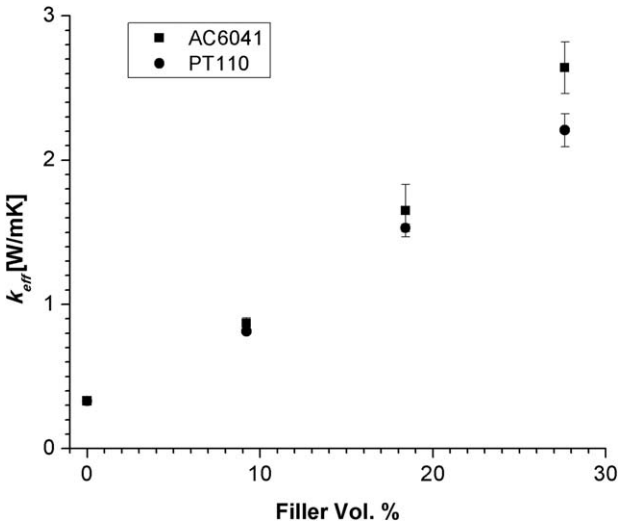

Figure 2. Effects of hBN platelet sizes and contents on the LDPE-hBN composite's k_{eff}.

with 9.21 vol % of hBN loading, a sudden change in the material structure (i.e., formation of interconnected filler network) at hBN loading close to 10 vol % was suggested by a previous research.[38] Furthermore, the LDPE-hBN composite filled with 27.63 vol % of hBN demonstrated clear evidence of filler interconnection with the measured k_{eff} values. In order to explore how foam expansion could promote the formation of filler network, foamed PMCs with both 9.21 vol % and 27.63 vol % of hBN loading were studied in greater details and presented in following sections. Moreover, the measured k_{eff} of solid PMCs would also be used as a base case to evaluate the feasibility and effectiveness of foaming-assisted filler alignment to promote PMC's k_{eff}, especially for PMC with low filler loadings.

Effect of Volume Expansion of PMC Foams on their k_{eff}

Thermally conductive thermoplastic-ceramic composite foams with lower mass density and similar k_{eff} comparing with their solid counterparts had recently been reported.[32] However, to the best knowledge of the authors, PMC foams with their k_{eff} higher than solid PMC with the same filler loadings have never been achieved. In this context, a series of parametric studies were conducted to systematically elucidate the underlying mechanisms for the cellular morphology of a PMC foam influences the foam's k_{eff}.

LDPE-hBN composites filled with different hBN loadings and hBN platelets of different sizes were foamed to investigate the effect of volume expansion percent on PMC foam's k_{eff}. Figure 3 shows the representative SEM micrographs of these LDPE-hBN foams. Figure 3(a,b) illustrate that the microscale hBN_{PT110} platelets and submicron-scale hBN_{AC6041} platelets were preferentially aligned around expanded microspheres in LDPE-hBN foams. Both samples were foamed by 2.5× Expancel® microspheres to volume expansions of 25%. While hBN platelets were randomly oriented in the LDPE matrix, the expansion of microspheres generated biaxial stretching along their cell walls, and thereby induced the preferential alignment of the platelets along the cell walls around expanded microspheres. It can be observed

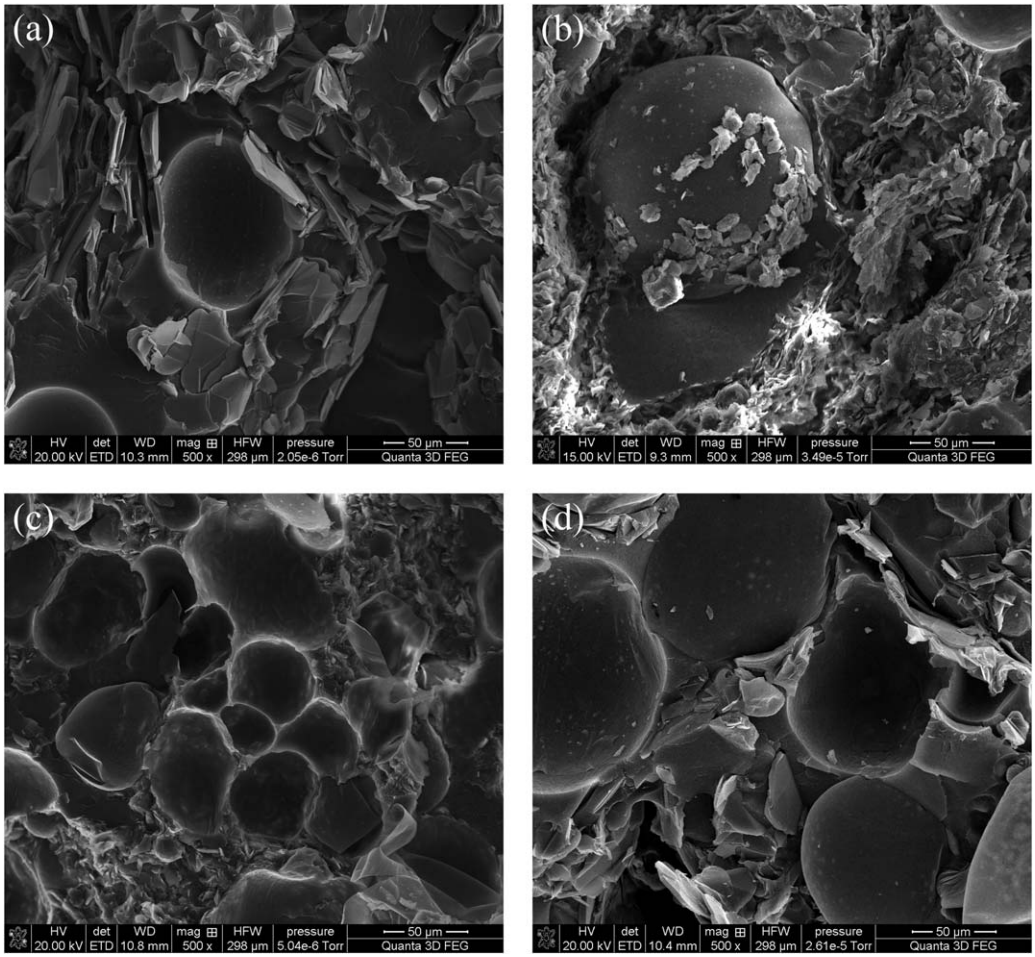

Figure 3. SEM micrographs of LDPE-hBN composite foams filled with 9.21 vol % hBN and 2.5× of Expancel® microspheres: (a) hBN_{PT110} & 25% volume expansion; (b) hBN_{AC6041} & 25% volume expansion; (c) hBN_{AC6041} & 75% volume expansion; and (d) hBN_{PT110} & 75% volume expansion.

that the submicron-scale platelets were able to form a more interconnected thermally conductive network than the micron-scale platelets. This can be attributed to the significantly larger (i.e., slightly over 13-fold) specific surface area of the submicron-scale platelets than that of the micron-scale platelets. Figure 3(c,d) depict that, for PMC foams filled with either hBN_{PT110} or hBN_{AC6041}, increasing the volume expansion percent from 25% to 75% would potentially block the formation of thermally conductive pathway because of the close proximity of adjacent expanded microspheres.

Figure 4 plots the effect of volume expansion percent on k_{eff} of LDPE-hBN foams filled with different types or loadings of hBN platelets. At 9.21 vol % filler loading, moderate foam expansion (e.g., 25%) of LDPE-hBN foams filled with either hBN_{PT110} or hBN_{AC6041} platelets enhanced the PMC's k_{eff}. In contrast, volume expansions beyond 50% were detrimental to the PMC foam's k_{eff}. For PMC foams with 25% volume expansion, the k_{eff} of LDPE-hBN foam filled with hBN_{AC6041} platelets was 1.16 W m^{-1} K^{-1}, which represented a 26% increase over that of its solid counterparts. The improved k_{eff} for LDPE-hBN foam filled with 9.21 vol % of hBN_{PT110} platelets and a volume expansion percent of 25% was 0.97 W m^{-1} K^{-1}, which was equivalent to a 21% increase over that of the solid composite. These results represent the first time PMC foams with their k_{eff} higher than solid PMC embedded with the same filler loadings were fabricated. The more pronounced positive effect of moderate foam expansion on k_{eff} of PMC filled with hBN_{AC6041} could be caused by the higher efficiency of submicron-scale hBN platelets to establish interconnecting filler network in the LDPE matrix. One-way ANOVA tests were conducted to verify the dependence of PMC foams' k_{eff} on the foams' volume expansion percent. Table VI summarized the statistical results of the one-way ANOVA tests. The results indicate that the effect of PMC foam's volume expansion percent on the foam's k_{eff} was significant for PMC foams filled with 9.21 vol %, hBN_{AC6041}, 9.21 vol % hBN_{PT110}, and 27.63 vol % hBN_{AC6041}. The mound-shape k_{eff} - to-volume expansion relationship reveals that there would be two or more competing factors that governed PMC foam's k_{eff}. Unlike LDPE-hBN foams filled with 9.21 vol % hBN platelets, the k_{eff} of PMC foams loaded with 27.63 vol % hBN_{AC6041} platelets decreased monotonically as their volume expansion percent increased.

For LDPE-hBN foams filled with 9.21 vol % hBN platelets, the positive effects of foaming on PMC's k_{eff} include (i) foaming-assisted filler alignment along the cell walls [i.e., Figure 3(a,b)]; and (ii) localization of hBN platelets in the solid phase of the

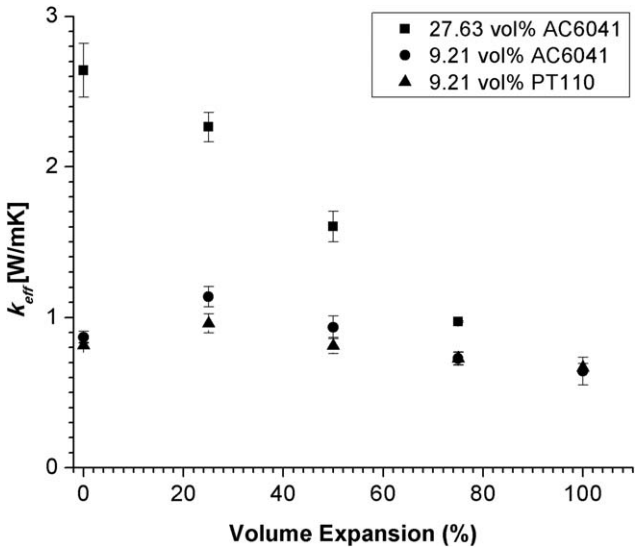

Figure 4. Effect of volume expansion % on k_{eff} of LDPE-hBN composite foamed by 2.5× Expancel® microspheres.

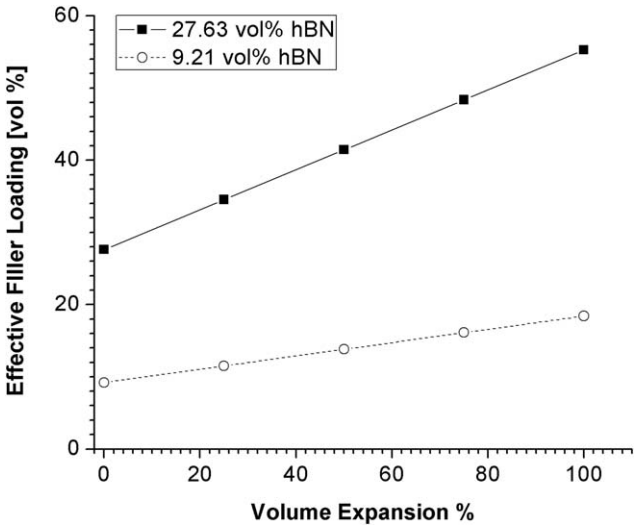

Figure 5. Effective filler loading with respect to different volume expansion %.

PMC foam. The effective filler content in the PMC foam's solid region can be determined by eq. (5):

$$\text{Effective filler content} = \frac{\phi_{\text{filler}}(V_{\text{solid}} + V_{\text{void}})}{V_{\text{solid}}} \times 100\% \quad (5)$$

where ϕ_{filler} is the volume fraction of hBN platelets in the PMC, V_{solid} is the volume of the solid phase in the PMC foam, and V_{void} is the total volume of all voids in the PMC foam.

The presence of foaming-induced filler alignment was evident in Figure 3(a,b). The preferential orientation of hBN platelets along the cell wall of expanded microspheres would promote the interconnectivity of the hBN platelets, leading to a positive impact on the PMC foam's k_{eff}. Figure 5 shows how PMC foam's volume expansion would increase the effective filler content in the solid phase. For example, a 25% volume expansion of LDPE-hBN foams filled with 9.21 vol % hBN platelets would result in an effective hBN content of 11.51 vol %. Such hBN platelets localization in the LDPE matrix would result in a higher probability of filler networking, and thereby promoting the PMC foam's k_{eff}.

In contrast, the negative influence of foaming on LDPE-hBN composite foam's k_{eff} could be attributed to (i) the introduction of thermally insulating voids in the polymer matrix; and (ii) the disruption of hBN filler network between adjacent cells. It is obvious that increasing PMC foam's volume expansion percent would raise the volume fraction of thermally insulating voids, and be detrimental to the PMC's k_{eff}. Moreover, as indicated in Figure 3(c), close proximity of expanded microspheres in excessively expanded PMC foams would disrupt the establishment of hBN filler network. This would also have a negative impact on the PMC's k_{eff}. At 27.63 vol % hBN loading, the omnipresence of hBN platelets had guaranteed an excessive interconnected hBN network in the LDPE matrix. Therefore, further increase in effective filler concentration in localized region would have minimal impact on further promoting filler interconnectivity, and thereby overall thermally conductive network. This explains why the PMC's k_{eff} decreased monotonically as the volume expansion percent and the fraction of thermally insulating voids increased.

Table VI. One-Way ANOVA Tests for the Dependence of PMC Foams' k_{eff} on PMC Foam's Volume Expansion Percent

Testing parameter	Data set	*P*	Significance (%)
Volume Expansion %	9.21 vol % hBN_{AC6041}	7.2×10^{-7}	>99
	9.21 vol % hBN_{PT110}	8.8×10^{-5}	>99
	27.63 vol % hBN_{AC6041}	1.1×10^{-6}	>99

Effect of Cell Size of PMC Foams on their k_{eff}

Using the methods described in the experimental section, PMC foams were fabricated to study the effect of cell size on the k_{eff} of PMC foams at four levels of volume expansion percent (i.e., 25%, 50%, 75%, and 100%). Figure 6 plotted the measured k_{eff} of LDPE-hBN_{AC6041} with 9.21 vol % of hBN platelets and controlled foam expansion percent against cell size. For the LDPE-hBN_{AC6041} foams with 25% and 50% volume expansion, it was observed that the PMC foam's k_{eff} can be promoted by a moderate amount of cell size growth; whereas excessive cell expansion would lead to a reduced k_{eff}. In contrast, the k_{eff} of PMC foams with volume expansion of 75% and 100% seems to be insensitive to the change in cell size. One-way ANOVA tests have been performed, and the results are summarized in Table VII. It is verified that the effect of filler size on PMC foam's k_{eff} is significant for PMC foams with volume expansion of 25% and 50%.

The mound-shape k_{eff} -to-cell size relationship that possessed by PMC foams with 25% and 50% volume expansion suggested that cell growth would bring both positive and negative effects

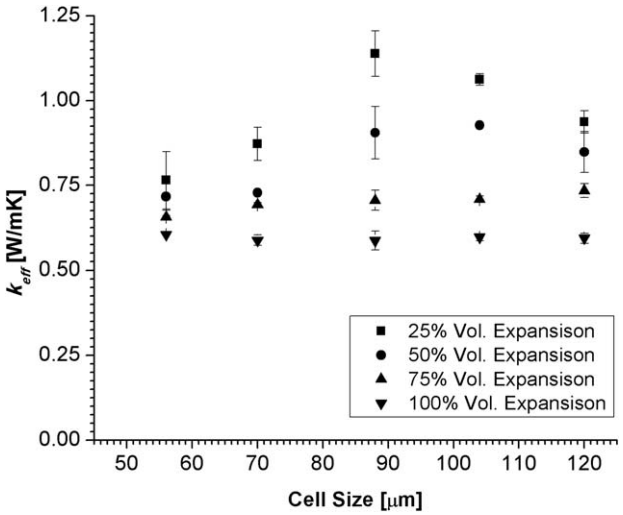

Figure 6. Effect of cell size on the k_{eff} of LDPE-hBN$_{AC6041}$ foams filled with 9.21 vol % hBN and with different volume expansion %.

on the PMC foam's k_{eff}. At each constant volume expansion percent, the effect of filler localization induced by foam expansion in the solid phase would be comparable. Therefore, the positive effect was solely attributed to the different levels of cell expansion-induced biaxial stress field, which helps hBN platelets align around the cell wall. Such preferential alignment and enhanced networking of submicron-scale hBN platelets by foaming in a LDPE matrix is illustrated in Figure 7. This observation was consistent with other studies on foaming-induced enhancement in PMC's mechanical or electrical properties.[21,43] The foaming-induced biaxial stress field increased with bubble expansion, and thereby resulting in higher degree of filler alignment along the cell wall to establish a thermally conductive network. However, once the cell expansion reached the critical level (i.e., most hBN platelets become preferentially aligned tangentially around the expanded microspheres, further biaxial stretch would potentially result in the breaking of thermally conductive network, and suppressing the PMC foam's k_{eff} as illustrated with the schematics in Figure 8. This phenomenon is consistent with similar observations in electrically conductive polymer-carbon nanotubes nanocomposites.[43]

Secondly, the difference in the sensitivity of PMC foam's k_{eff} on cell size indicated that cell expansion-induced effects are more

Table VII. One-Way ANOVA Tests for the Dependence of PMC Foams' k_{eff} on PMC Foam's Cell Size

Testing parameter	Data set	*P*	Significance (%)
Cell size	25% volume expansion	7.9×10^{-4}	>99
	50% volume expansion	3.0×10^{-3}	>99
	75% volume expansion	0.043	>95
	100% volume expansion	0.828	<18

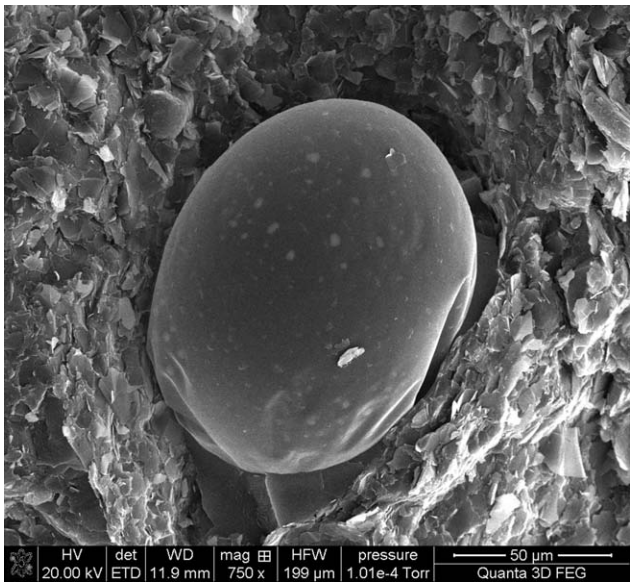

Figure 7. Foaming-assisted alignment of hBN$_{AC6041}$ platelets around an expanded bubble in a 25% expanded PMC foam (with 9.21 vol % hBN$_{AC6041}$ & 2.5× Expancel® microspheres).

significant in PMC foams with low volume expansion percent. When the PMC foam has high volume expansion percent, the high volume fraction of thermally insulating air voids became the predominant factor on the PMC foam's k_{eff}. This phenomenon could be attributed to the blockage of filler network, as illustrated in Figure 3(c). Considering the air voids have a simple cubic arrangement, eq. (6) was used to determine the average cell-to-cell distance. The calculated cell-to-cell distance under different volume expansion percent and cell sizes are summarized in Table VIII.

$$D=\left(\sqrt[3]{\left(\frac{VE\%+1}{VE\%}\right)\frac{\pi}{6}}-1\right)\cdot d \quad (6)$$

where D is the average cell-to-cell distance, VE % is the volume expansion %, and d is the average cell size.

For PMC foams with low volume expansion (i.e. 25% and 50%), the estimated cell-to-cell distances were relatively large. For these foams, the aforementioned positive and negative effects of cell size contributed to the mound-shaped curve. However, as the PMC foam's volume expansion increased, adjacent cells became closer to each other. For example, the estimated cell-to-cell distances were less than 2 μm for PMC foams with 100% volume expansion. Therefore, with the random dispersion of the microspheres in the LDPE matrix, it was highly probable that cells would be in contact with each other and completely avoid the formation of a thermally conductive path in some regions (as shown in Figure 3(c)). This significantly suppressed the PMC foam's k_{eff}, and the influence of cell size on PMC foams' k_{eff} became negligible.

Effect of Cell Population Density of PMCs on their k_{eff}

In order to study the effect of cell population density on the PMC foam's k_{eff}, PMC foams filled with 9.21 vol % of hBN$_{AC6041}$ and with different volume expansion percent were fabricated with two different cell population densities by

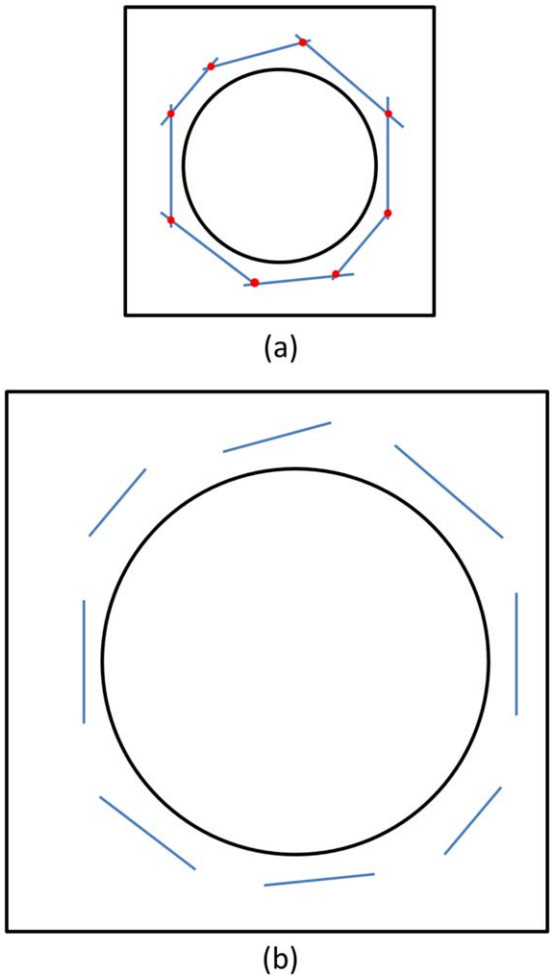

Figure 8. Schematics of cell expansion-induced filler connection disruption: (a) enhanced filler connection by foaming-induced filler alignment; and (b) filler disconnection induced by excessive cell expansion. [Color figure can be viewed in the online issue, which is available at wileyonlinelibrary.com.]

changing the amount of Expancel® microspheres (i.e., 0.029 g/cm^3 and 0.058 g/cm^3 with respect to the solid volume) being embedded in the LDPE matrices. Figure 9 plotted the k_{eff} of PMC foams at two different levels of cell population density

Table VIII. Theoretically Calculated Average Cell-to-Cell Distance under Different Combination of Expancel® Loading and Volume Expansion Percent

	Average cell-to-cell distance (μm)			
Average cell size (μm)	25% Volume expansion	50% Volume expansion	75% Volume expansion	100% Volume expansion
120	45.4	19.4	8.2	1.86
104	39.6	17.0	7.2	1.62
88	33.4	14.4	6.2	1.36
70	26.6	11.4	4.8	1.08
56	21.0	9.0	3.8	0.86

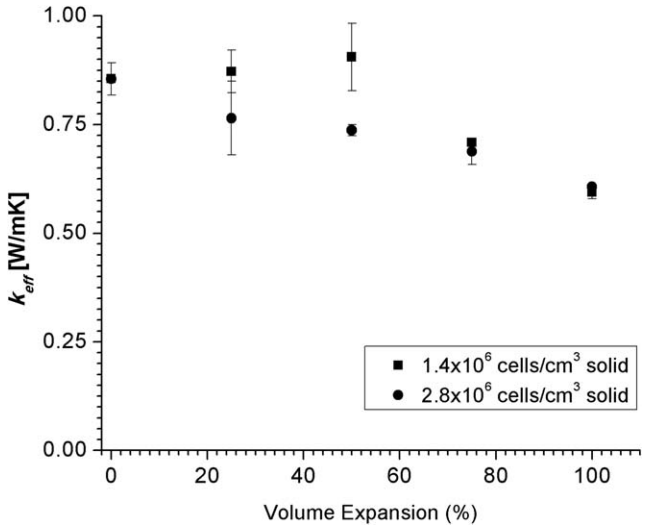

Figure 9. Effect of cell population density on the LDPE-hBN$_{AC6041}$ composite's k_{eff}.

(i.e., 1.4 × 10^6 cells/cm^3 and 2.8 × 10^6 cells/cm^3 with respect to unfoamed volume) against different levels of volume expansions. Experimental results revealed that the dependences of PMC foam's k_{eff} on the volume expansion percent were different for foams with different cell population densities. It was found that the PMC foams with lower cell population density (i.e., 1.4 × 10^6 cells/cm^3 with respect to unfoamed volume) had a mound-shaped k_{eff} -to-volume expansion relationship and the maximum k_{eff} occurred at approximately 50% volume expansion. In contrast, the k_{eff} of PMC foams with cell density of 2.8 × 10^6 cells/cm^3 with respect to unfoamed volume showed a monotonically decreasing trend. Overall, it can be observed that the k_{eff} of PMC foams with volume expansion of 75% and 100% seems to be insensitive to the change in cell population. One-way ANOVA tests have been performed, and the results are summarized in Table IX. It is verified that the effect of cell population density on PMC foam's k_{eff} is significant for PMC foams with volume expansion of 25% and 50%.

In order to understand the different behaviors caused by these two levels of cell densities, it must be noted that the three morphological parameters, cell size, volume expansion percent, and cell population density are interrelated. In other words, each of

Table IX. One-Way ANOVA Test for the Dependence of PMC Foams' k_{eff} on PMC Foam's Cell Population Density

Testing parameter	Data set	*P*	Significance (%)
Cell Population Density	25% volume expansion	0.130	87
	50% volume expansion	0.094	>90
	75% volume expansion	0.906	<10
	100% volume expansion	0.553	<50

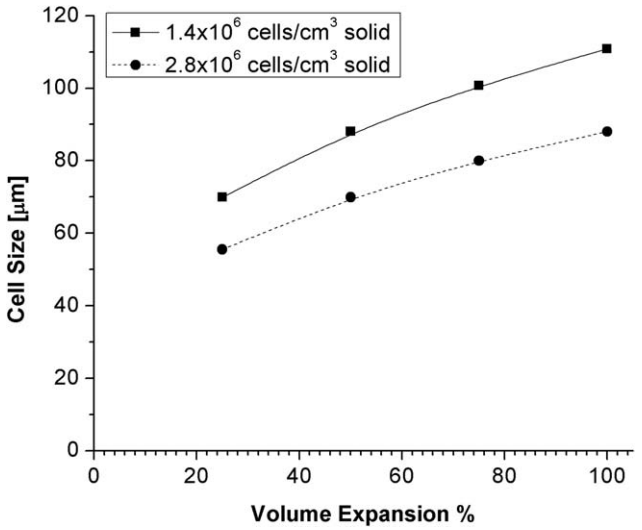

Figure 10. Effect of foam volume expansion on the average cell size with constant cell population density.

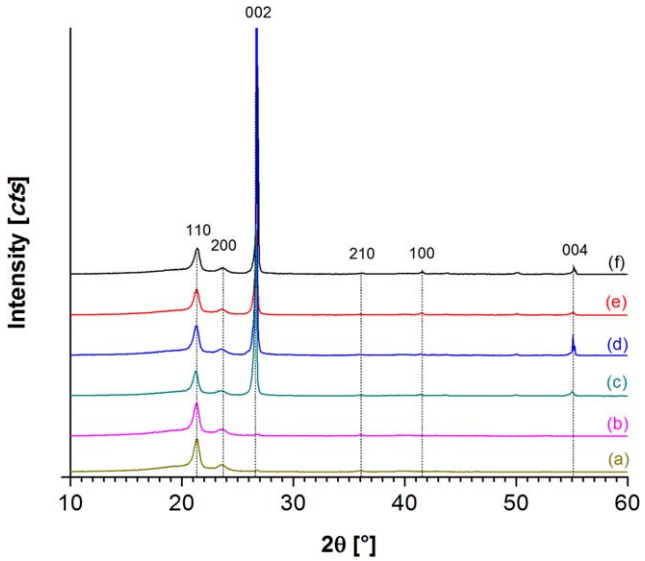

Figure 11. XRD spectra of the LDPE, LDPE-hBN composites, and their foams: (a) neat LDPE; (b) LDPE foam with 25% volume expansion; (c) LDPE-hBN_{AC6041} solid composite with 9.21 vol % hBN; (d) LDPE-hBN_{PT110} solid composite with 9.21 vol % hBN; (e) LDPE-hBN_{AC6041} composite foam with 9.21 vol % hBN and 25% volume expansion; and (f) LDPE-hBN_{PT110} composite foam with 9.21 vol % hBN and 25% volume expansion. [Color figure can be viewed in the online issue, which is available at wileyonlinelibrary.com.]

the three parameters is determined simultaneously by the other two. Moreover, to increase volume expansion percent without changing the cell population density, the average cell size also needs to be increased. At a fixed cell population density, the average cell size can be calculated as a function of volume expansion percent using eq. (7). Figure 10 plotted the calculated average cell size as a function of the foam's volume expansion percent at the aforementioned two levels of cell population densities.

$$d=\sqrt[3]{\frac{6\times VE\%}{\pi N}} \tag{7}$$

where d is the average cell size, VE % is the volume expansion %, and N is the number of cells per unit volume of solid.

For the PMC foams with a cell population density of 1.4×10^6 cells/cm^3 with respect to unfoamed volume, the cell size increased from approximately 70 μm to 111 μm as the volume expansion percent varied from 25% to 100%. The maximum k_{eff} occurred at 50% volume expansion. Figure 10 showed that the corresponding cell size is around 88 μm, which was consistent with the result in Figure 6. In other words, the initial increasing trend could be attributed to the cell expansion-induced filler alignment, as discussed in Effect of Cell Size of PMC Foam on their k_{eff} section. As the volume expansion percent continued to increase, the corresponding average cell size became larger. As discussed in Effects of Volume Expansion of PMC Foam on their k_{eff} and Effect of Cell Size of PMC Foam on their k_{eff} sections, both excess foam expansion and cell size could disrupt the filler interconnectivity. Together with the large volume fraction of thermally insulating air, the PMC foam's k_{eff} dropped after reaching its peak at 50% volume expansion.

For the PMC foams with a cell density of 2.8×10^6 cells/cm^3 with respect to unfoamed volume, as the volume expansion increased from 25% to 100%, the corresponding cell size increased from approximately 55 μm to 88 μm. In this case, the average cell sizes were smaller than that of the PMC foams with a cell density of 1.4×10^6 cells/cm^3 with respect to unfoamed volume under same volume expansion percent. For instance, the average cell size was only 55 μm for PMC foams with 25% volume expansion. The low degree of cell expansion was not sufficient to effectively align the hBN platelets along the cell wall. When the optimal cell size of about 88 μm had been reached, the corresponding volume expansion was 100%. The high volume fraction of thermally insulating air and the challenge to form an interconnected conductive filler path due to the small cell-to-cell distance would suppress the k_{eff}.

Effects of hBN and Foam Expansion on the Crystalline Structures of the LDPE and LDPE Composites

As shown in Figure 11, typical crystalline peaks of LDPE at 21.5°, 24.3°, and 36.5° were observed from the X-ray diffraction

Table X. Effects of hBN and Foam Expansion on the XRD Spectra of LDPE, LDPE-hBN Composites, and their Foams (25% Volume Expansion)

Composition	Peak	FWHM (°)	Peak area (°·cts)	Crystallite size (Å)
Neat LDPE	(110)	0.1181	367.87	676.87
LDPE Foam	(110)	0.1378	394.29	580.11
LDPE-hBN_{AC6041} Composite	(110)	0.3936	862.26	203.07
LDPE-hBN_{PT110} Composite	(110)	0.1968	529.72	406.15
LDPE-hBN_{AC6041} Composite Foam	(110)	0.4330	1062.8	184.62
LDPE-hBN_{PT110} Composite Foam	(110)	0.3936	928.13	203.11

Table XI. Effects of Filler Size and Foam Expansion on the XRD Spectra of LDPE, LDPE-hBN Composites, and their Foams (25% Volume Expansion)

Composition	Peak	FWHM (°)	Peak Area (°·cts)	Crystallite Size (Å)
LDPE-hBN_{AC6041} Composite	(002)	0.1378	18645.68	585.85
LDPE-hBN_{PT110} Composite	(002)	0.0787	67028.77	1025.92
LDPE-hBN_{AC6041} Composite Foam	(002)	0.1771	9296.68	455.90
LDPE-hBN_{PT110} Composite Foam	(002)	0.1378	24326.56	586.03
LDPE-hBN_{AC6041} Composite	(004)	0.1680	503.64	527.21
LDPE-hBN_{PT110} Composite	(004)	0.0590	2291.83	1501.62
LDPE-hBN_{AC6041} Composite Foam	(004)	0.4320	282.96	205.07
LDPE-hBN_{PT110} Composite Foam	(004)	0.0720	841.11	1231.01
LDPE-hBN_{AC6041} Composite	(100)	0.1968	125.85	426.80
LDPE-hBN_{PT110} Composite	(100)	0.1968	94.31	426.78
LDPE-hBN_{AC6041} Composite Foam	(100)	0.2362	192.2	355.68
LDPE-hBN_{PT110} Composite Foam	(100)	0.1968	205.15	426.94

(XRD) spectra of LDPE and LDPE composites, which corresponded to the orthorhombic crystallite plane 110, 200, 210, respectively.[44] The XRD spectra reveal that the addition of Expancel® and/or hBN increased both the area and full width at half maximum (FWHM) of the (110) peak, which correspond to an increase in the degree of crystalline phase and a decrease in the crystal size. Table X shows that the area of the (110) peak increased most significantly in LDPE-hBN composite foams, followed by solid LDPE-hBN composites, and then LDPE foam. This is attributed to the synergistic effect of two mechanisms, (i) stress-induced crystallization caused by the extensional stress generated around expanding bubbles,[45] and (ii) enhanced crystallization by the presence of hBN platelets as the nucleating agent.[46] Furthermore, the effect of filler-induced crystallization was observed to be more prominent when smaller hBN platelets (i.e., AC6041) were used.

The typical (002), (004), and (100) peaks in an XRD spectrum of hBN were found in LDPE-hBN composites in Figure 11.[47] The (002) and (004) peaks refer to horizontally oriented hBN (i.e., the through-plane of hBN is perpendicular to the horizontal direction) while the (100) peak is related to vertically oriented hBN.[48] Table XI shows the effects of hBN platelet size and foam expansion on the XRD spectra of LDPE composites. As expected, larger hBN platelets (i.e., PT110) resulted in stronger intensities and larger crystalline sizes for the (002) and (004) peaks due to the significant difference in the lateral sizes of the two hBN grades. Comparing with the solid LDPE-hBN composites, the dramatically change of the intensities of (002), (004) and (100) peaks of LDPE-hBN composite foams provide evidence of the foaming-induced change in hBN orientation in the composites.

CONCLUSIONS

This study has successfully fabricated thermally conductive low density polyethylene (LDPE)-hexagonal boron nitride (hBN) composite foams with their effective thermal conductivity (k_{eff}) higher than their solid counterparts. In order to explore how foaming induced filler alignment can promote the formation of such filler network, PMC foams with two levels of filler loading (i.e., 9.21 and 27.63 vol %) were studied. In particular, the k_{eff} of PMC foams filled with 9.21 vol % of hBN_{AC6041} (i.e., submicron-scale) or hBN_{PT110} (i.e., micron-scale) reached as high as 1.16 W m^{-1} K^{-1} and 0.97 W m^{-1} K^{-1}, respectively. These values represented 26% and 21% increases over those of their solid counterparts. Parametric studies were conducted to study the effects of foam morphologies on the PMC foam's k_{eff}.

It was found that both foam volume expansion and cell size had competing effects on the PMC foam's k_{eff}. PMC foams with moderate volume expansion percent would promote the foams' k_{eff}. This was caused by the localization of fillers in the solid phase, which promoted the hBN platelets' interconnectivity. In contrast, high volume expansion percent would result in high volume fraction of thermally insulating air voids. The reduced average cell-to-cell distance would also disrupt the development of continuous thermally conductive path. Therefore, the PMC foam's k_{eff} would decrease. Similarly, large cell sizes also had both beneficial and detrimental effects on the k_{eff}. On the one hand, cell expansion would create a biaxial stress field that promoted filler alignment along the cell walls, and promoted the PMC foam's k_{eff}. On the other hand, excessive cell expansion could disrupt the development of interconnected filler network, and subsequently suppress the PMC foam's k_{eff}. Furthermore, the enhancement of LDPE crystallization by the synergistic effect of the presence of hBN platelets and the foaming-induced crystal nucleation was shown in X-ray diffraction (XRD) analyses. The XRD spectra also reveal foam expansion led to changes in the orientation of hBN platelets.

In short, the findings of this research provided guidelines for the design and fabrication of lightweight thermally conductive PMC foams. Such thermally-conductive PMC foams would provide a new material family to assist the industry to deal with the challenge in heat management problem in their next generation products.

REFERENCES

1. Mack, C. A. *IEEE Trans. Semicond. Manuf.* **2011**, *24*, 202.
2. Beanato, G.; Giovannini, P.; Cevrero, A.; Athanasopoulos, P.; Zervas, M.; Temiz, Y.; Temiz, Y. *IEEE J. Emerg. Sel Topic Circuits Syst.* **2012**, *2*, 295.

3. Manzione, L. T. Plastic Packaging of Microelectronic Devices; Van Nostrand: New York, **1990**.
4. Mamunya, Y. P.; Davydenko, V. V.; Pissis, P.; Lebedev, E. V. *Eur. Polym. J.* **2002**, *38*, 1887.
5. Tekce, H. T.; Kumlutas, D.; TavmanI, I. H. *J. Reinforced Plast. Comp.* **2007**, *26*, 113.
6. Yung, K. C.; Liem, H. *J. Appl. Polym. Sci.* **2007**, *106*, 3587.
7. Leung, S. N.; Khan, M. O.; Chan, E.; Naguib, H. E.; Dawson, F.; Adinkrah, V.; Lakatos-Hayward, L. *J. Appl. Polym. Sci.* **2013**, *127*, 3293.
8. King, J.; Johnson, B. A.; Via, M. D.; Ciarkowski, C. J. *Polym. Compos.* **2010**, *31*, 497.
9. Tu, H.; Ye, L. *J. Appl. Polym. Sci.* **2010**, *116*, 2336.
10. Agari, Y.; Ueda, A.; Tanaka, M.; Nagai, S. *J. Appl. Polym. Sci.* **1990**, *40*, 929.
11. Lee, E.; Lee, S.; Shanefield, D.; Cannon, W. *J. Am. Ceram. Soc.* **2008**, *91*, 1169.
12. Ishida, H.; Rimdusit, S. *Thermochim. Acta* **1998**, *320*, 177.
13. Bigg, D. *Adv. Polym. Sci.* **1995**, *119*, 1.
14. Haggenmueller, R.; Guthy, C.; Lukes, J. R.; Fischer, J. E.; Winey, K. I. *Macromolecules* **2007**, *40*, 2417.
15. Kalaitzidou, K.; Fukushima, H.; Drzal, L. T. *Carbon* **2007**, *45*, 1446.
16. Berman, R. *Contemp. Phys.* **1973**, *14*, 101.
17. Tsutsumi, N.; Takeuchi, N.; Kiyotsukuri, T. *J Polym. Sci. Part B: Polym. Phys.* **1991**, *29*, 1085.
18. Martin, C. A.; Sandler, J. K. W.; Windle, A. H.; Schwarz, M. K.; Bauhofer, W.; Schulte, K.; Shaffer, M. P. *Polymer* **2005**, *46*, 877.
19. Leung, S. N.; Khan, M. O.; Naguib, H. E.; Dawson, F. *Appl. Phys. Lett.* **2014**, *104*, 081904.
20. Yu, A.; Ramesh, P.; Sun, X.; Bekyarova, E.; Itkis, M. E.; Haddon, R. C. *Adv. Mater.* **2008**, *20*, 4740.
21. Okamoto, M.; Nam, P. H.; Maiti, M.; Nakayama, T.; Takada, M.; Okamoto, H. *Nano Lett.* **2001**, *1*, 503.
22. Han, S. J.; Lee, H. I.; Jeong, H. M.; Kim, B. K.; Raghu, A. V.; Reddy, K. R. *J. Macromol. Sci. Part B: Phys.* **2014**, *53*, 1193.
23. Reddy, K. R.; Jeong, H. M.; Lee, Y.; Raghu, A. V. *J. Polym. Sci. Part A: Polym. Chem.* **2010**, *48*, 1477.
24. Reddy, K. R.; Sin, B. C.; Ryu, K. S.; Kim, J. C.; Chung, H.; Lee, Y. *Synth. Met.* **2009**, *159*, 595.
25. Seki, N.; Arai, T.; Suzuki, Y.; Kawakami, H. *Polymer* **2012**, *53*, 2062.
26. Hassan, M.; Reddy, K. R.; Haque, E.; Faisal, S. N.; Ghasemi, S.; Minett, A. I.; Gomes, V. G. *Compos. Sci. Technol.* **2014**, *98*, 1.
27. Mota-Morales, J. D.; Gutiérrez, M. C.; Ferrer, M. L.; Jiménez, R.; Santiago, P.; Sanchez, I. C.; Terrones, M.; Del Monte, F.; Luna-Bárcenas, G. *J. Mater. Chem. A.* **2013**, *1*, 3970.
28. hoi, C.; Kim, S. H.; Raghu, D. H.; Reddy, A. V.; Lee, K. R.; Yoon, H. I.; Jeong, K. S.; Ki, H. M. B. K. *J. Macromol. Sci. Part B: Phys.* **2012**, *51*, 197.
29. Lobos, J.; Velankar, S. *J. Cellul. Plast.* to appear, DOI: 10.1177/0021955X14546015.
30. Ameli, A.; Jung, P. U.; Park, C. B. *Carbon* **2013**, *60*, 379.
31. Yan, D. X.; Dai, K.; Xiang, Z. D.; Li, Z. M.; Ji, X.; Zhang, W. Q. *J. Appl. Polym. Sci.* **2011**, *120*, 3014.
32. Chan, E.; Leung, S. N.; Khan, M. O.; Naguib, H. E.; Dawson, F.; Adinkrah, V. *Macromol. Mater. Eng.* **2012**, *297*, 1014.
33. Ding, H.; Leung, S. N. *J. Cellul. Plast.* to appear, DOI: 10.1177/0021955X14566211.
34. Leung, S. N.; Wong, A.; Leung, L. C.; Park, C. B. *J. Supercrit. Fluids* **2012**, *63*, 187.
35. Naguib, H. E.; Park, C. B.; Reichelt, N. *J. Appl. Polym. Sci.* **2004**, *91*, 2661.
36. Raman, C.; Meneghetti, P. *Plast. Addit. Compd.* **2008**, *10*, 26.
37. Engler, M.; Uibel, K.; Eichler, J. *U. S. Pat. 12/964195*, December 09, **2012**.
38. Leung, S. N.; Ghaffari, S.; Naguib, H. E. Behavior and Mechanics of Multifunctional Materials and Composites; Proceeding of SPIE: San Diego, CA, **2013**, *8689*, 86890F.
39. ASTM International. ASM E1225-04. ASTM International: West Conshohocken, **2004**.
40. Scherrer, P. *Nachr. Ges. Wiss. Göttingen* **1918**, *26*, 98.
41. Agari, Y.; Udeda, A.; Nagai, S. *J. Appl. Polym. Sci.* **1991**, *42*, 1665.
42. Swartz, E. T.; Pohl, R. O. *Appl. Phys. Lett.* **1987**, *51*, 2200.
43. Ameli, A.; Nofar, M.; Park, C. B.; Potschke, P.; Rizvi, G. *Carbon* **2014**, *71*, 206.
44. Murray, K. A.; Kennedy, J. E.; McEvoy, B.; Vrain, O.; Ryan, D.; Cowman, R.; Higginbo, C. L. *Int. J. Mater. Sci.* **2013**, *3*, 1.
45. Wong, A.; Guo, Y.; Park, C. B. *J. Supercrit. Fluids* **2013**, *79*, 142.
46. Kai, W.; He, Y.; Inoue, Y. *Polym. Int.* **2005**, *54*, 780.
47. Li, L.; Glushenkov, A. M.; Hait, S. K.; Hodgson, P.; Chen, Y. *Sci. Rep.* **2014**, *4*, 7288.
48. Lin, Z. Functionalized Graphene for Energy Storage and Conversion; PhD Dissertation. Georgia Institute of Technology: Atlanta, GA, **2014**.